Available online at www.sciencedirect.com

SciVerse ScienceDirect

Current Opinion in Structural Biology

Structural biology *in situ* — the potential of subtomogram averaging

John AG Briggs

Cryo-electron tomography provides low-resolution 3D views of cells, organelles, or viruses. Macromolecular complexes present in multiple copies can be subsequently identified within the 3D reconstruction (the tomogram), computationally extracted, and averaged to obtain higher resolution 3D structures, as well as a map of their spatial distribution. This method, called subtomogram averaging or subvolume averaging, allows structures of macromolecular complexes to be resolved *in situ*. Recent applications have provided *in situ* structural data at resolutions of 2–4 nm on samples including polysomes, nuclear pores, vesicle coats, and viral surface proteins. Here I describe the method and discuss limitations, advances and recent applications. I speculate how the method will solve more structures at higher resolution, allowing *in situ* structural biology.

Address
Structural and Computational Biology Unit, European Molecular Biology Laboratory, Meyerhofstrasse 1, 69117 Heidelberg, Germany

Corresponding author: Briggs, John AG (john.briggs@embl.de)

Current Opinion in Structural Biology 2013, **23**:261–267

This review comes from a themed issue on **Macromolecular assemblies**

Edited by **Felix Rey** and **Wesley I Sundquist**

For a complete overview see the Issue and the Editorial

Available online 4th March 2013

0959-440X/$ – see front matter,

http://dx.doi.org/10.1016/j.sbi.2013.02.003

Introduction

Visualizing the structure of macromolecular assemblies in three dimensions can provide direct insights into function and mechanism. Visualizing structure can also have wider and subtler impact: it influences how researchers think about biological problems, how they develop hypotheses, and how they design experiments to address function. The majority of structural biology methods require the purification of macromolecular complexes, and their subsequent study in solution or after crystallization. In order to fully understand how macromolecules function it would be much better if we could resolve their structure *in situ*, in their cellular context, without purification. We would see the range of conformations adopted by the complex, its interaction partners, and its position relative to cellular organelles, other complexes, and other copies of itself. Methods for resolving the structure of macromolecular complexes *in situ* therefore have enormous potential. Cryo-electron tomography combined with image processing using subtomogram averaging methods can provide detailed 3D information on the structure of macromolecular complexes *in situ*. In this review I will discuss the basic principles of subtomogram averaging, what it can be used for, its potential and limitations, and I will give examples of research areas where the method has already had major impact.

The basic principles of the method

Subtomogram averaging incorporates features of cryo-electron tomography and single particle reconstruction. The basic principle is as follows: multiple copies of a macromolecular complex of interest are identified from within a 3D cryo-electron tomography reconstruction and subtomograms that contain the complex of interest are cut-out, aligned and averaged together to obtain an isotropic, 3D structure of the complex. This principle is expanded upon here, relating subtomogram averaging to cryo-electron microscopy, tomography and single particle image processing.

Single particle cryo electron microscopy and cryo-electron tomography both make use of transmission electron microscopes to generate projection images of biological samples. The samples have been vitrified — that is they have been frozen with sufficient speed, or under sufficient pressure, that crystalline ice has not formed, but the sample is instead preserved in a glass-like vitreous state. In order for the electron beam to pass through the biological sample and generate a projection image, the sample must be thin, typically less than 500 nm. If the sample is not thin to start with (such as a thin layer of buffer, or the thin protrusions of a cell), then sections of the sample can be cut using a microtome ('vitreous-sectioning' [1]) or thin lamella can be generated by using a focused ion beam to mill away surrounding material [2]. Biological samples are easily damaged by the electron beam, and for this reason only very low electron doses can be used for imaging. As when taking photos at twilight without a flash, this results in images that have very low signal-to-noise ratios.

In single-particle cryo-electron microscopy (for a recent review see [3]). the sample is a thin layer of a buffer solution containing the macromolecular complex of interest. Although the signal-to-noise ratio of each image is low, images of many different copies of the macromolecular complex can be collected, and these can be averaged

together to obtain better signal-to-noise and better resolution. Since the complexes are often randomly oriented within the sample, the dataset will contain images showing the complex viewed from all directions. Combining many thousands of such images allows a high-resolution three-dimensional reconstruction of the complex to be obtained.

In cryo-electron tomography (for a recent review see [4]) the sample is a unique object: part of a cell, a heterogeneous virus particle or an organelle. In order to view the sample from different directions the sample is physically rotated within the electron microscope and images are collected at different rotation angles. Combining these images allows a three-dimensional reconstruction to be obtained. The total electron dose that the sample can tolerate is divided over all of the collected images, and the images therefore have an even lower signal-to-noise ratio than the images used in single-particle cryo-electron microscopy. The information in a typical cryo-electron tomogram can be reliably interpreted only to a resolution of approximately 5 nm. Because the sample cannot be rotated through a full 180° in the electron microscope (the sample holder at some point obscures the beam), some views are missing, and the resolution of the reconstruction is lower parallel to the beam than in other directions. This is known as the 'missing-wedge problem' because in Fourier space the missing information has the shape of a wedge. Since the sample is a pleomorphic object (*e.g.* a cell), it is not possible to average many images of different copies of the sample to increase the signal-to-noise and therefore the resolution. The cell might, however, contain multiple identical copies of certain macromolecular complexes.

Single-particle averaging methods can generally not be applied to average these complexes because the projection image of the complex of interest *in situ* is obscured by all of the other objects above and below it in the sample that superimpose in the image. In some cases the complex of interest may be bound to another heterogenous feature in the sample, for example ribosomes bound to the endoplasmic reticulum, which also hinders single-particle averaging. In the 3D reconstruction from a cryo-electron tomogram, the 3D nature of the information removes the super-position problem and macromolecular complexes can more easily be identified. Where many copies of the macromolecular complex of interest are found within the tomograms, these can be extracted in 3D, aligned to a reference and averaged together (Figure 1) (see also [5]). A classification step may also be included to identify only those complexes in a particular conformation. The alignment process is iterative: the subtomograms are aligned against a reference structure, then averaged to generate a new structure, and this new structure is used as a reference for alignment of the subtomograms (Figure 1). This procedure can be iterated until the structure no longer changes. Averaging improves the signal-to-noise and therefore the resolution. Further, since the different

Figure 1

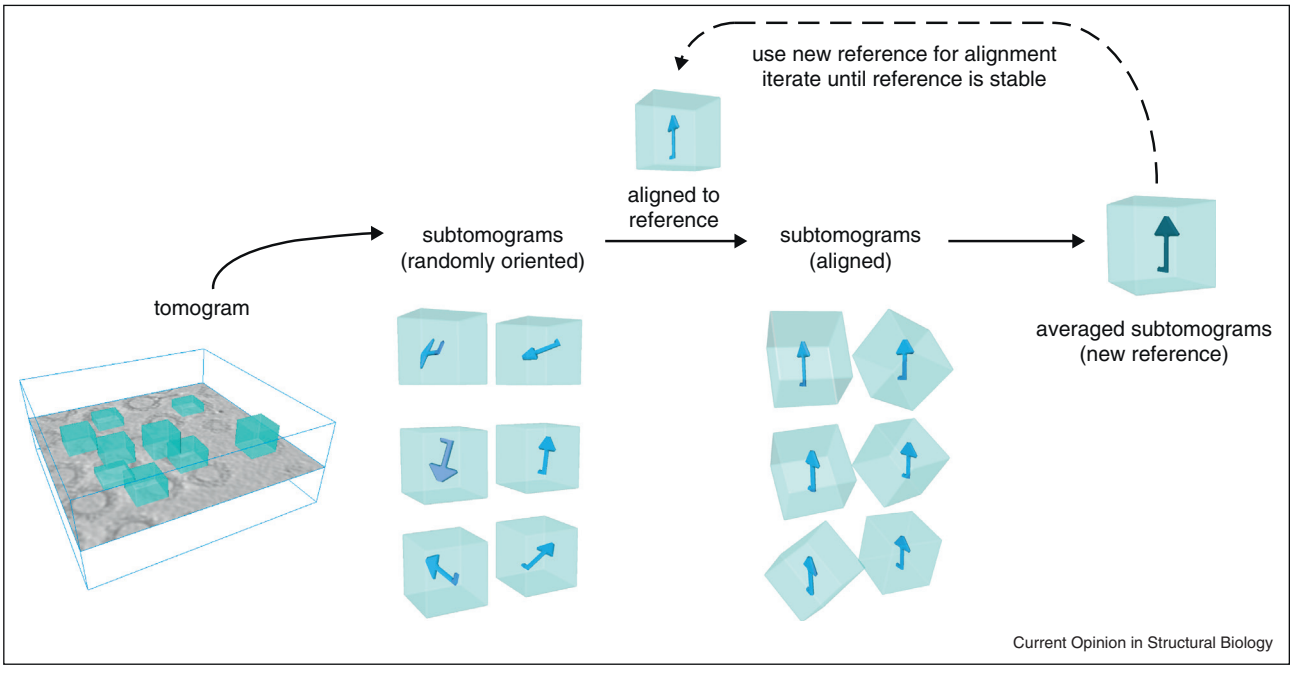

An overview of subtomogram averaging in its simplest form. Subtomograms are extracted from the tomogram. They are rotationally and translationally aligned against a reference. The aligned subtomograms are then averaged to generate a new reference. The new reference is then used for alignment of the subtomograms again. This procedure is repeated until the reference stabilizes.

copies of the complex are oriented differently relative to the missing wedge of information, the final reconstruction has higher-resolution in all directions. In this way subtomogram averaging can be used to obtain 3D structural information. The 3D structure, however, is not the only information that is obtained. The positions at which the complex of interest was found within the tomogram, together with information from the alignment step, defines the relative positions and orientations of the different copies of the complex. Subtomogram averaging can therefore be used both to resolve the structure of a complex *in situ*, and also to understand the spatial distribution and relative spatial relationships of the copies of the complex.

The limitations of the method

In order to be able to carry out subtomogram averaging, a number of conditions need to be fulfilled. Firstly, the macromolecular complex must be present in multiple copies within the tomographic dataset. Secondly, it must be possible to locate and orient the complex within the tomogram. To do this the object must be sufficiently large and have strong enough low-resolution features to be distinguishable from surrounding objects. The majority of successful applications of subtomogram averaging focused on large complexes located inside cells or organelles (typically above ~750 kDa), small complexes located on the surface of viruses or vesicles (typically above ~300 kDa), or smaller complexes that assemble into regular arrays where the feature which is identified is an oligomer (such as viral structural lattices or chemoceptor arrays). Thirdly, the object must show limited structural heterogeneity so that at least a sub-population with a conserved conformation can be identified and averaged.

The resolution that can be obtained is dependent on a number of factors: firstly, the number of copies of the object which can be included in the reconstruction (more subtomograms generally gives higher resolution); secondly, the structural flexibility of the complex (an object which is highly flexible will only be reconstructed to low resolution); thirdly the thickness of the sample (thinner objects give higher signal-to-noise in the tomogram which is reflected in improved alignments and higher resolution). The highest-resolution *de novo* structures obtained by subtomogram averaging had resolutions of around 2 nm. This does not, however, represent a resolution limit: refinements in image processing combined with better samples are likely to yield structures at higher-resolution over the coming years.

As for single particle EM, caution should be taken to validate the structure resulting from subtomogram averaging. Potential sources of error may include reference-bias and over-alignment, both of which can be avoided. In reference bias, the structure has features of the initial reference used for alignment that are not true features of the data. Reference bias can be avoided by using a cautious starting model (such as noise), by checking that different starting references give the same final model, or by using a starting reference of relatively low resolution while recovering high-resolution information in the final structure. In over-alignment, repeated iterations of alignment and averaging give a structure containing high-resolution features resulting from the alignment of noise against itself in a reinforcing manner. Over-alignment can be avoided by using references that contain only lower-resolution information at all iterations of alignment, while recovering higher-resolution information in the final structure. Alternatively, over-alignment can be avoided by treating two halves of the data independently — carrying out completely independent alignments against independent references — and by subsequently verifying that the two independent alignments converge to the same structure at all interpreted resolutions.

Application of the method: success stories

Over recent years, the application of subtomogram averaging methods has had a major impact in a number of fields (Figure 2). Studies have revealed the architecture and arrangement of polysomes [6,7], virus surface glycoproteins [8,9,10•,11], internal virus structural proteins [12–18], flagella [19], microtubule binding proteins [20], nuclear pore complexes [21–23], the mitochondrial F1Fo-ATPase [24••], respiratory chain complexes [25], chromatin [26], chemoreceptor arrays [27,28], desmosome plaques [29•] and coated trafficking vesicles [30••]. It is of note that many of these applications involve membrane bound complexes which are particularly challenging to study by other structural biology methods. The list above is far from complete. Here I briefly describe some of these examples.

Virus proteins *in situ*

Subtomogram averaging has been used to resolve the structures of surface proteins from enveloped viruses *in situ*. The small size of the virus particles allows thin samples to be prepared, and facilitates large data-collections, so studies of viruses have yielded some of the highest resolution subtomogram structures to date. Studies of the HIV glycoprotein alone or in complex with antibodies have allowed the description of open and closed conformations of the glycoprotein spike at ~2 nm resolution, and have defined antibody binding sites [9,10•,11]. Studies of a hantavirus revealed unexpected patches of tetrameric envelope protein complexes arranged in a square lattice [8]. These small lattice patches may play a role in mediating membrane curvature.

Subtomogram averaging has also been applied to the helical nucleocapsids of negative stranded RNA viruses. In studies of Marburg virus [12], and Measles virus [16], the Nucleocapsid was found to form a helix with a helical

Figure 2

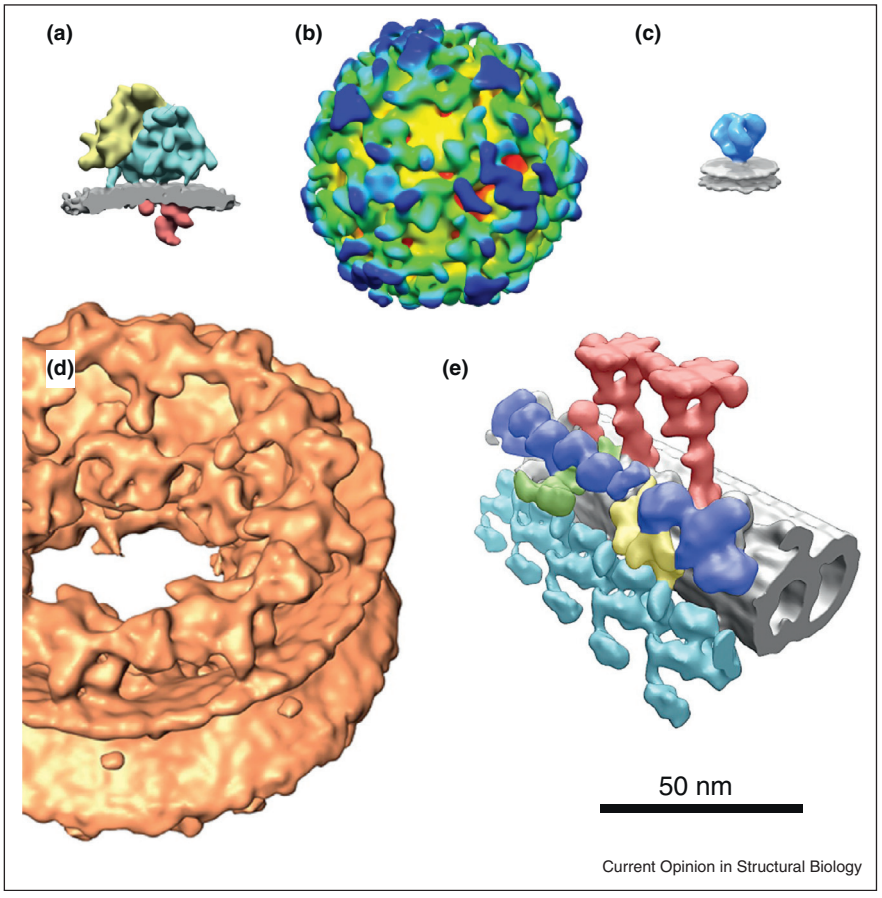

Examples of recent structures solved by subtomogram averaging, shown approximately to scale. **(a)** Ribosomes on the ER membrane [46••]. **(b)** COPI coated vesicles [30••]. **(c)** The glycoprotein spike of HIV [11]. **(d)** The human nuclear pore [23]. **(e)** A microtubule doublet from a Chlamydomonas flagellum [36]. Panels were adapted from the original references. Panel e © 2011 Rockefeller University Press. Originally published in Journal of Cell Biology. 195:673–687. http://dx.doi.org/10.1083/jcb.201106125.

symmetry that differed from the adjacent matrix layer with which the nucleocapsid interacts. The Marburg virus study was extended to look at nucleocapsids during assembly within infected cells. By applying subtomogram averaging to specific regions of nucleocapsids at different stages of budding, it was shown that the nucleocapsid adopts its mature assembled state before being wrapped in its membrane envelope [12].

The structural protein lattice of immature HIV has also been studied by subtomogram averaging, allowing approximate positioning of protein domains, as well as showing the overall arrangement of the proteins within the virus [13,17]. These studies led to a model of HIV assembly where the structural protein, Gag, forms a hexameric lattice that becomes curved by the incorporation of irregularly shaped defects. The lattice is incomplete, containing a large gap at the point at which the immature virus particle underwent membrane scission to release it from the infected cell. By studying structural changes in virus particles containing mutations limiting proteolytic maturation of the virus, the role of individual proteolytic sites in disassembling the immature lattice was explored [14,15,18].

Flagella, cilia and microtubules

The arrangement of microtubules and their associated proteins in flagella and cilia has been explored by a series of subtomogram averaging studies of flagella, both purified and *in situ* (see also [31]). The central axoneme of the flagella contains nine microtubule doublets arranged in a circle around a central microtubule pair. Dyneins mediate sliding of the doublets against one another to bend the flagella. Subtomogram averaging has been used to generate 3D reconstructions of flagella in the 3–4 nm resolution range [32–34,35•,36,37•]. By comparing the structures of flagella from wild-type cells with flagella from mutants lacking particular proteins, the positions of individual proteins have been defined, and compared between different doublets within the axoneme

[37•,38,39], as well as between axonemes from different organisms [40]. By understanding the arrangement of proteins on and between the microtubules in the axoneme it is hoped that models describing the mechanism of bending can be derived. Subtomogram averaging is also being applied to related areas such as the arrangement of proteins in the basal body [41,42], or in the ventral disc of Giardia [43].

Coated vesicles

Cages assembled from the outer coat proteins of the COPII and clathrin vesicular coats had previously been studied by single-particle electron microscopy revealing beautiful geometric cage structures [44,45]. We recently used subtomogram averaging to resolve the structure of the COPI coat on vesicles assembled *in vitro* [30••]. This approach allowed the coat structure to be visualized in the context of all of the protein components as well as the underlying membrane. The subtomogram averaging approach revealed not only the structure of the repetitive building block of the coat, but also its arrangement over the surface of each vesicle. We found that coatomer, the basic building block of the cage, was able to interact with either one or two copies of itself, depending on its position within the coat. We were then able to use the spatial distribution information from the subtomogram averaging to extract new subtomograms from the positions where different interactions were found, and to average them to resolve the 3D structure of the interacting regions. By combining the different structures with the spatial distributions calculated for individual vesicles it was possible to produce structural models of individual coated vesicles.

Ribosomes *in situ*

Purified ribsomes have been one of the most favoured objects for study by single particle cryo-electron microscopy, allowing the ribosome structure to be resolved to resolutions of less than 1 nm. Subtomogram averaging has been used to look at the structure and distribution of ribosomes within intact human cells [6]. The structure of the ribosome was resolved in this way to 4 nm. More revealing was that multiple ribosomes translating single mRNAs were arranged in preferred orientations relative to one another. These orientations were similar to those previously described in a similar study on bacterial polysomes in lysates [7], and they were specific to actively translating ribosomes. It remains unclear why adjacent ribosomes on the chain have preferred relative orientations, but the conservation of the arrangements between bacteria and mammals suggests a critical function. The arrangement may prevent interactions between adjacent nascent polypeptide chains, or serve to protect the mRNA under certain conditions.

The application of subtomogram averaging to ribosomes on the surface of ER-derived microsomes yielded a structure at ~3 nm resolution [46••]. This revealed that the ES27L ribosomal subunit forms a bridging density between the ribosome and the ER membrane, and showed the presence of lumenal densities, which likely correspond to ribosome-associated complexes. As in cytosolic polysomes, the ER associated ribosomes had a preferred arrangement relative to one another, which may facilitate the simultaneous translation of an mRNA by multiple ribosomes. Together these studies shed first light on the structure and defined arrangements of ribosomes *in situ*: further studies of translating ribosomes *in situ* are now required to understand the functional significance of these arrangements.

The nuclear pore

The nuclear pore from an *amoeba* was one of the first structures described using subtomogram averaging methods [21,47]. More recently, structures have been solved for frog [22] and human [23] nuclear pores at around 6.5 nm resolution. The general structure of an eight-fold ring is conserved, but the metazoan pores are taller than those of the *amoeba*. In all cases the pores are not perfectly circular, and therefore the eight asymmetric units are aligned and averaged separately. The low resolution of the pore structures, as compared to other structures solved by subtomogram averaging, is likely to reflect a combination of several unfavorable factors including thick samples, relatively small datasets, and inherent flexibility within the pore.

Hybrid image processing methods

Subtomogram averaging can also been incorporated into hybrid image processing methods. In single-particle reconstruction methods, obtaining a reliable initial 3D model of the structure from 2D projections is often challenging, and 3D subtomogram alignment may be one avenue to generate such starting models. Subtomogram averaging has also been used to measure the shape of tubular protein arrays, and the arrangement of proteins within the arrays for subsequent reconstruction from 2D images by helical/single particle reconstruction methods [12,48••]. We used such an approach to resolve the arrangement of capsid proteins in *in vitro* assembled tubular arrays that mimic the immature state of retroviruses [48••] — subtomogram averaging was used to determine the helical symmetry parameters of individual tubes, 2D helical reconstruction was then used to solve their structures, and 3D subvolume averaging to combine data from multiple tubes. The final 8 Å structure revealed regions of the protein involved in retrovirus assembly, and the structural changes associated with maturation of retroviruses into the infectious form.

The future

Subtomogram averaging is currently unique in its power to describe the structure and the spatial arrangement of macromolecular complexes *in situ*. Over the coming years

I expect that the number of labs applying these methods will increase, and also that the power of the method to address difficult problems will increase. There are a number of factors that will contribute to this expansion. Firstly, the efficiency of sample preparation methods will improve, allowing thin sections or lamella to be robustly produced from thick vitrified cells thereby permitting a wider number of targets to be addressed. Secondly, electron microscope hardware improvements, in particular the combination of direct-electron detectors and energy filters, will lead to collection of higher signal-to noise data. This will permit robust alignment of smaller objects from thicker samples, and will decrease the amount of data required to obtain a given resolution. Thirdly, data collection routines will continue to be optimized, leading to collection of datasets that are larger, datasets from which critical microscope parameters such as defocus are known or can be reliably determined and datasets which have the optimal conditions of dose, focus, and geometry for the problem being addressed. Fourthly, powerful and increasing user-friendly software for the alignment of tomographic series and of subtomograms is being developed and will continue to be developed (*e.g.* [49••,50,51]), making subtomogram averaging more accessible, while also improving the quality of alignment and classification of the data.

Subtomogram averaging is a relatively young method, and there remain many avenues for optimization, as well as many unexplored applications. By revealing the structure of macromolecular complexes *in situ* it can have major impact on our understanding of biological mechanism and function.

Acknowledgements

I thank Juha Huiskonen and Martin Beck for insightful comments that helped to improve the manuscript.

References and recommended reading

Papers of particular interest, published within the period of review, have been highlighted as:

- • of special interest
- •• of outstanding interest

1. Al-Amoudi A, Chang JJ, Leforestier A, McDowall A, Salamin LM, Norlen LP, Richter K, Blanc NS, Studer D, Dubochet J: **Cryo-electron microscopy of vitreous sections**. *EMBO J* 2004, **23**:3583-3588.
2. Rigort A, Villa E, Bauerlein FJ, Engel BD, Plitzko JM: **Integrative approaches for cellular cryo-electron tomography: correlative imaging and focused ion beam micromachining**. *Methods Cell Biol* 2012, **111**:259-281.
3. Lau WC, Rubinstein JL: **Single particle electron microscopy**. *Methods Mol Biol* 2013, **955**:401-426.
4. Yahav T, Maimon T, Grossman E, Dahan I, Medalia O: **Cryo-electron tomography: gaining insight into cellular processes by structural approaches**. *Curr Opin Struct Biol* 2011, **21**:670-677.
5. Schmid MF: **Single-particle electron cryotomography (cryoET)**. *Adv Protein Chem Struct Biol* 2011, **82**:37-65.
6. Brandt F, Carlson LA, Hartl FU, Baumeister W, Grunewald K: **The three-dimensional organization of polyribosomes in intact human cells**. *Mol Cell* 2010, **39**:560-569.
7. Brandt F, Etchells SA, Ortiz JO, Elcock AH, Hartl FU, Baumeister W: **The native 3D organization of bacterial polysomes**. *Cell* 2009, **136**:261-271.
8. Huiskonen JT, Hepojoki J, Laurinmaki P, Vaheri A, Lankinen H, Butcher SJ, Grunewald K: **Electron cryotomography of Tula hantavirus suggests a unique assembly paradigm for enveloped viruses**. *J Virol* 2010, **84**:4889-4897.
9. Liu J, Bartesaghi A, Borgnia MJ, Sapiro G, Subramaniam S: **Molecular architecture of native HIV-1 gp120 trimers**. *Nature* 2008, **455**:109-113.
10. • Tran EE, Borgnia MJ, Kuybeda O, Schauder DM, Bartesaghi A, Frank GA, Sapiro G, Milne JL, Subramaniam S: **Structural mechanism of trimeric HIV-1 envelope glycoprotein activation**. *PLoS Pathog* 2012, **8**:e1002797.
This study addresses the structure of the HIV envelope glycoprotein bound to antibodies and receptors. It is a good illustration of the use of subtomogram averaging to resolve multiple different structural states of a system and thereby generate mechanistic insight.
11. White TA, Bartesaghi A, Borgnia MJ, Meyerson JR, de la Cruz MJ, Bess JW, Nandwani R, Hoxie JA, Lifson JD, Milne JL *et al.*: **Molecular architectures of trimeric SIV and HIV-1 envelope glycoproteins on intact viruses: strain-dependent variation in quaternary structure**. *PLoS Pathog* 2010, **6**:e1001249.
12. Bharat TA, Riches JD, Kolesnikova L, Welsch S, Krahling V, Davey N, Parsy ML, Becker S, Briggs JA: **Cryo-electron tomography of Marburg virus particles and their morphogenesis within infected cells**. *PLoS Biol* 2011, **9**:e1001196.
13. Briggs JA, Riches JD, Glass B, Bartonova V, Zanetti G, Krausslich HG: **Structure and assembly of immature HIV**. *Proc Natl Acad Sci U S A* 2009, **106**:11090-11095.
14. Carlson LA, de Marco A, Oberwinkler H, Habermann A, Briggs JA, Krausslich HG, Grunewald K: **Cryo electron tomography of native HIV-1 budding sites**. *PLoS Pathog* 2010, **6**:e1001173.
15. de Marco A, Muller B, Glass B, Riches JD, Krausslich HG, Briggs JA: **Structural analysis of HIV-1 maturation using cryo-electron tomography**. *PLoS Pathog* 2010, **6**:e1001215.
16. Liljeroos L, Huiskonen JT, Ora A, Susi P, Butcher SJ: **Electron cryotomography of measles virus reveals how matrix protein coats the ribonucleocapsid within intact virions**. *Proc Natl Acad Sci U S A* 2011, **108**:18085-18090.
17. Wright ER, Schooler JB, Ding HJ, Kieffer C, Fillmore C, Sundquist WI, Jensen GJ: **Electron cryotomography of immature HIV-1 virions reveals the structure of the CA and SP1 Gag shells**. *EMBO J* 2007, **26**:2218-2226.
18. Keller PW, Adamson CS, Heymann JB, Freed EO, Steven AC: **HIV-1 maturation inhibitor bevirimat stabilizes the immature Gag lattice**. *J Virol* 2011, **85**:1420-1428.
19. Bui KH, Pigino G, Ishikawa T: **Three-dimensional structural analysis of eukaryotic flagella/cilia by electron cryo-tomography**. *J Synchrotron Radiat* 2011, **18**:2-5.
20. Cope J, Gilbert S, Rayment I, Mastronarde D, Hoenger A: **Cryo-electron tomography of microtubule–kinesin motor complexes**. *J Struct Biol* 2010, **170**:257-265.
21. Beck M, Lucic V, Forster F, Baumeister W, Medalia O: **Snapshots of nuclear pore complexes in action captured by cryo-electron tomography**. *Nature* 2007, **449**:611-615.
22. Frenkiel-Krispin D, Maco B, Aebi U, Medalia O: **Structural analysis of a metazoan nuclear pore complex reveals a fused concentric ring architecture**. *J Mol Biol* 2010, **395**:578-586.
23. Maimon T, Elad N, Dahan I, Medalia O: **The human nuclear pore complex as revealed by cryo-electron tomography**. *Structure* 2012, **20**:998-1006.
24. •• Davies KM, Anselmi C, Wittig I, Faraldo-Gomez JD, Kuhlbrandt W: **Structure of the yeast F1Fo-ATP synthase dimer and its role in shaping the mitochondrial cristae**. *Proc Natl Acad Sci U S A* 2012, **109**:13602-13607.

The structure of the F1Fo-ATP synthase dimer solved from mitochondrial cristae shows interactions at the base of the peripheral stalks, defining the relative orientation of the two monomers. This study highlights the importance of *in situ* studies to define physiological context-dependent interactions between complexes that may not be well preserved *in vitro*.

25. Dudkina NV, Kudryashev M, Stahlberg H, Boekema EJ: **Interaction of complexes I, III, and IV within the bovine respirasome by single particle cryoelectron tomography**. *Proc Natl Acad Sci U S A* 2011, **108**:15196-15200.

26. Scheffer MP, Eltsov M, Frangakis AS: **Evidence for short-range helical order in the 30-nm chromatin fibers of erythrocyte nuclei**. *Proc Natl Acad Sci U S A* 2011, **108**:16992-16997.

27. Briegel A, Li X, Bilwes AM, Hughes KT, Jensen GJ, Crane BR: **Bacterial chemoreceptor arrays are hexagonally packed trimers of receptor dimers networked by rings of kinase and coupling proteins**. *Proc Natl Acad Sci U S A* 2012, **109**:3766-3771.

28. Liu J, Hu B, Morado DR, Jani S, Manson MD, Margolin W: **Molecular architecture of chemoreceptor arrays revealed by cryoelectron tomography of *Escherichia coli* minicells**. *Proc Natl Acad Sci U S A* 2012, **109**:E1481-E1488.

29. • Al-Amoudi A, Castano-Diez D, Devos DP, Russell RB, Johnson GT, Frangakis AS: **The three-dimensional molecular structure of the desmosomal plaque**. *Proc Natl Acad Sci U S A* 2011, **108**:6480-6485.

In this manuscript subtomogram averaging is used to obtain a 3D view of the roughly periodic arrangement of proteins within the desmosomal plaque. The samples are prepared by vitreous sectioning of human skin. The study illustrates the potential of subtomogram averaging to obtain structural data within tissue.

30. •• Faini M, Prinz S, Beck R, Schorb M, Riches JD, Bacia K, Brugger B, Wieland FT, Briggs JA: **The structures of COPI-coated vesicles reveal alternate coatomer conformations and interactions**. *Science* 2012, **336**:1451-1454.

By applying subtomogram averaging to coated membrane vesicles, this study showed that conformational heterogeneity of the coat protein complex is a key feature of assembly of the COPI coat. The study made use of the spatial distribution of the protein identified by subtomogram averaging to return to the data and extract and average regions where particular interactions between complexes occurred.

31. Nicastro D: **Cryo-electron microscope tomography to study axonemal organization**. *Methods Cell Biol* 2009, **91**:1-39.

32. Bui KH, Sakakibara H, Movassagh T, Oiwa K, Ishikawa T: **Asymmetry of inner dynein arms and inter-doublet links in Chlamydomonas flagella**. *J Cell Biol* 2009, **186**:437-446.

33. Hoog JL, Bouchet-Marquis C, McIntosh JR, Hoenger A, Gull K: **Cryo-electron tomography and 3-D analysis of the intact flagellum in *Trypanosoma brucei***. *J Struct Biol* 2012, **178**:189-198.

34. Koyfman AY, Schmid MF, Gheiratmand L, Fu CJ, Khant HA, Huang D, He CY, Chiu W: **Structure of *Trypanosoma brucei* flagellum accounts for its bihelical motion**. *Proc Natl Acad Sci U S A* 2011, **108**:11105-11108.

35. • Nicastro D, Fu X, Heuser T, Tso A, Porter ME, Linck RW: **Cryo-electron tomography reveals conserved features of doublet microtubules in flagella**. *Proc Natl Acad Sci U S A* 2011, **108**:E845-E853.

This study generated a 3 nm resolution isotropic structure of the microtubule doublet in flagella, clarifying the connectivity of components and drawing attention to the complicated arrangements of density inside the microtubules.

36. Pigino G, Bui KH, Maheshwari A, Lupetti P, Diener D, Ishikawa T: **Cryoelectron tomography of radial spokes in cilia and flagella**. *J Cell Biol* 2011, **195**:673-687.

37. • Bui KH, Yagi T, Yamamoto R, Kamiya R, Ishikawa T: **Polarity and asymmetry in the arrangement of dynein and related structures in the Chlamydomonas axoneme**. *J Cell Biol* 2012, **198**:913-925.

This study describes the variation in arrangement of proteins between different radial and longitudinal positions within the axoneme. This asymmetry will be critical to the mechanism of flagella bending

38. Heuser T, Barber CF, Lin J, Krell J, Rebesco M, Porter ME, Nicastro D: **Cryoelectron tomography reveals doublet-specific structures and unique interactions in the I1 dynein**. *Proc Natl Acad Sci U S A* 2012, **109**:E2067-E2076.

39. Lin J, Heuser T, Song K, Fu X, Nicastro D: **One of the nine doublet microtubules of eukaryotic flagella exhibits unique and partially conserved structures**. *PLoS ONE* 2012, **7**:e46494.

40. Pigino G, Maheshwari A, Bui KH, Shingyoji C, Kamimura S, Ishikawa T: **Comparative structural analysis of eukaryotic flagella and cilia from Chlamydomonas, Tetrahymena, and sea urchins**. *J Struct Biol* 2012, **178**:199-206.

41. Li S, Fernandez JJ, Marshall WF, Agard DA: **Three-dimensional structure of basal body triplet revealed by electron cryo-tomography**. *EMBO J* 2012, **31**:552-562.

42. Guichard P, Desfosses A, Maheshwari A, Hachet V, Dietrich C, Brune A, Ishikawa T, Sachse C, Gonczy P: **Cartwheel architecture of Trichonympha basal body**. *Science* 2012, **337**:553.

43. Schwartz CL, Heumann JM, Dawson SC, Hoenger A: **A detailed, hierarchical study of Giardia lamblia's ventral disc reveals novel microtubule-associated protein complexes**. *PLoS ONE* 2012, **7**:e43783.

44. Fotin A, Cheng Y, Grigorieff N, Walz T, Harrison SC, Kirchhausen T: **Structure of an auxilin-bound clathrin coat and its implications for the mechanism of uncoating**. *Nature* 2004, **432**:649-653.

45. Stagg SM, Gurkan C, Fowler DM, LaPointe P, Foss TR, Potter CS, Carragher B, Balch WE: **Structure of the Sec13/31 COPII coat cage**. *Nature* 2006, **439**:234-238.

46. •• Pfeffer S, Brandt F, Hrabe T, Lang S, Eibauer M, Zimmermann R, Forster F: **Structure and 3D arrangement of endoplasmic reticulum membrane-associated ribosomes**. *Structure* 2012, **20**:1508-1518.

The structure of ribosomes bound to the endoplasmic reticulum showed structural changes in the ribosome, the presence of associated lumenal densities, and a preferred relative arrangement of ribosomes on the surface of the membrane. Such studies will reveal the arrangement of ribosome associated proteins *in vivo*.

47. Beck M, Forster F, Ecke M, Plitzko JM, Melchior F, Gerisch G, Baumeister W, Medalia O: **Nuclear pore complex structure and dynamics revealed by cryoelectron tomography**. *Science* 2004, **306**:1387-1390.

48. •• Bharat TA, Davey NE, Ulbrich P, Riches JD, de Marco A, Rumlova M, Sachse C, Ruml T, Briggs JA: **Structure of the immature retroviral capsid at 8 Å resolution by cryo-electron microscopy**. *Nature* 2012, **487**:385-389.

In a hybrid approach, subtomogram averaging was used to determine the degree of distortion and the helical symmetry parameters of individual tubular protein arrays. These parameters were then used to reconstruct the same individual tubes from 2D images using helical reconstruction methods. Structures of unit cells from multiple individual tubes were then combined in a final 3D alignment and averaging step to give an 8 Å structure.

49. •• Castano-Diez D, Kudryashev M, Arheit M, Stahlberg H: **Dynamo: a flexible, user-friendly development tool for subtomogram averaging of cryo-EM data in high-performance computing environments**. *J Struct Biol* 2012, **178**:139-151.

This software is designed to be user-friendly, but also to be flexible, to make optimal use of computing resources, and importantly to interact easily with a range of other software packages and file formats used in subtomogram averaging. It is therefore an excellent example of the kind of software development that will open up subtomogram averaging to wider use.

50. Hrabe T, Chen Y, Pfeffer S, Cuellar LK, Mangold AV, Forster F: **PyTom: a python-based toolbox for localization of macromolecules in cryo-electron tomograms and subtomogram analysis**. *J Struct Biol* 2012, **178**:177-188.

51. Scheres SH, Melero R, Valle M, Carazo JM: **Averaging of electron subtomograms and random conical tilt reconstructions through likelihood optimization**. *Structure* 2009, **17**:1563-1572.